surfaces

MDPI

Article

Investigation of Photoelectron Properties of Polymer Films with Silicon Nanoparticles

Elizaveta A. Konstantinova [1,2,3,*], Alexander S. Vorontsov [1] and Pavel A. Forsh [1,2,3]

[1] Faculty of Physics, M.V. Lomonosov Moscow State University, Leninskie Gory 1-2, Moscow 119991, Russia; as.vorontsov@physics.msu.ru (A.S.V.); phorsh@mail.ru (P.A.F.)
[2] Department of Nano-, Bio-, Information Technology and Cognitive Science, Moscow Institute of Physics and Technology, Institutskij 9, Dolgoprudny, Moscow 141701, Russia
[3] National Research Center Kurchatov Institute, Akademika Kurchatova 1, Moscow 123182, Russia
* Correspondence: liza35@mail.ru

Received: 21 February 2019; Accepted: 11 May 2019; Published: 13 May 2019

Abstract: Hybrid samples consisting of polymer poly-3(hexylthiophene) (P3HT) and silicon nanoparticles were prepared. It was found that the obtained samples were polymer matrixes with conglomerates of silicon nanoparticles of different sizes (10–10^4 nm). It was found that, under illumination, the process of nonequilibrium charge carrier separation between the silicon nanoparticles and P3HT with subsequent localization of the hole in the polymer can be successfully detected using electron paramagnetic resonance (EPR) spectroscopy. It was established that the main type of paramagnetic centers in P3HT/silicon nanoparticles are positive polarons in P3HT. For comparison, samples consisting only of polymer and silicon nanoparticles were also investigated by the EPR technique. The polarons in the P3HT and P_b centers in the silicon nanoparticles were observed. The possibility of the conversion of solar energy into electric energy is shown using structures consisting of P3HT polymer and silicon nanoparticles prepared by different methods, including the electrochemical etching of a silicon single crystal in hydrofluoric acid solution and the laser ablation of single-crystal silicon in organic solvents. The results can be useful for solar cell development.

Keywords: polymer; silicon nanoparticles; EPR spectroscopy; photoconversion

1. Introduction

Solar cells based on crystalline or polycrystalline silicon are now the dominant technology globally [1–3]. However, the cost of such batteries is quite high, which is leading to the rapid development of technologies using amorphous silicon [4,5]. In addition to the low cost of devices, the use of amorphous silicon can decrease the thickness of solar cells, as well as their weight and material consumption, due to its higher absorption ability. However, the efficiency of solar cells based on amorphous silicon remains quite low, at 14%, compared to crystalline solar cells (approximately 25%) [6]. Increasing the efficiency of amorphous silicon-based solar cells is potentially possible using semiconductor nanocrystals. However, this is a very complex problem because it requires the development of methods for improving the injection and transport of charge carriers in such structures. Therefore, the development of cheap photo-electric converters has become a subject of great interest in the last years [1–4]. One of the perspective directions of the depreciation of phototransformation is the development of solar elements on the basis of polymers [7,8]. However, at the moment, the effectiveness of the phototransformation of such solar elements and their stability are low. The available literary data [7,9] demonstrate the prospects of use of hybrid structures on the basis of silicon nanoparticles (nc-Si) and organic compounds for transformation of solar energy. Such devices have the advantage of solution preparation but at the same time are characterized by

a much broader spectral range of absorption because of inorganic semiconductors. It should be borne in mind that the absorption coefficient of nc-Si with a diameter of about 10 nm and more is comparable with that of bulk Si. For small nc-Si with quantum confinement effects, the band gap strongly increases and the absorption coefficient grows. There have only been a few investigations of silicon/organic semiconductor heterojunctions for solar cells [7,9–11]. However, many questions concerning the correlation between the conditions of preparation of nc-Si and the electrophysical and optical properties of such hybrid structures still have no definite answer. Since point defects in solids are the centers of capture of charge carriers and limit the transport of charge carriers, their study is an important problem [12]. A powerful tool for studying the nature and properties of defects is electron paramagnetic resonance (EPR) spectroscopy [13]. The structure and properties of defects in nc-Si and other semiconductor nanoparticles have been successfully studied with EPR spectroscopy, taking advantage of the high specific area of these materials [13,14]. In spite of the different types of nc-Si structures, different preparation and storage conditions, the dominant type of defect (paramagnetic centers) in nc-Si is an Si dangling bond at the Si/SiO_2 interface or P_b center [14,15]. There are two types of P_b centers, P_{b0} (at the (111), (100) Si/SiO_2 interface) and P_{b1} (at the (100) Si/SiO_2 interface), which are characterized by different parameters of EPR spectra [14]. The P_b center concentration is very sensitive to vacuum heating and oxidation [14]. During vacuum heating (at temperatures higher than 300–400 °C), an Si dangling bond similar to that in amorphous silicon is detected in nc-Si [14]. A free electron EPR signal is observed in some samples of nc-Si [14]. EX center defects are detected in high-temperature oxidized nc-Si [14]. In poly-3(hexylthiophene) (P3HT), the main type of defect center is a positive polaron [9]. Therefore, in this work, we investigated the properties of defect states in hybrid samples consisting of polymer P3HT and silicon nanoparticles and in samples consisting only of polymer and silicon nanoparticles for comparison. We also measured the current–voltage characteristics of structures containing silicon nanocrystals in a polymeric matrix.

2. Experimental

Silicon nanoparticles were prepared by two methods [15,16]. The first method was the electrochemical etching of monocrystal plates of silicon of n-type of conduction in a solution of hydrofluoric acid (HF) and ethanol (C_2H_5OH). After etching, the samples were dried, and then silicon particles were removed from the plate mechanically (nc-Si(1)). The second method of manufacturing silicon nanoparticles (nc-Si(2)) was the pulse laser ablation of a substrate of monocrystal silicon in organic solvents (C_6H_5Cl, benzene chloride, and $CHCl_3$, chloroform). For the formation of the structures, the received nanoparticles were immediately added to the P3HT solution. Then, the resulting mixture was applied on the glass substrate containing an ITO layer as one of electrical contacts. The second was the aluminum contact which was sprayed from above onto the P3HT film. The current–voltage characteristics of the samples were measured using Keithley 6487.

The investigation of structure of the prepared samples was performed using scanning electronic microscopy (using a Carl Zeiss Supra 40-30-87 microscope, Oberkochen, Germany). The features of the internal structure of the polymer and the characteristics of the obtained silicon nanoparticles were determined by means of the Raman technique. For the Raman spectra registration, the Horiba Jobin Yvon HR800 spectrometer was used. A helium–neon laser (λ = 632.8 nm) was the source of light excitation. Raman signal recording was made in a configuration of reflection. A digital camera with a charge-coupled device (CCD) matrix was used as the detector. For the direct detection of separation processes of photoinduced charges in structures of nc-Si/P3HT, EPR spectroscopy was used. Measurements were performed using the Bruker EPR-spectrometer ELEXSYS-500, Rheinstetten, Germany (with a frequency of 9.5 GHz and a sensitivity of 5×10^{10} spin/mT). The EPR spectra simulation was carried out using the EasySpin MATLAB toolbox [17]. Illumination was carried out immediately in the spectrometer cavity by means of a mercury lamp with high pressure ($\Delta\lambda$ = 270–900 nanometers, power is 50 W).

3. Results and Discussions

Figure 1 shows an example of the structure of the nc-Si(1)/P3HT. Similar images were observed also for the other samples, nc-Si(2)/P3HT. According to Figure 1, the samples under investigation represent conglomerates of nanoparticles of various sizes (10–10^4 nm) dissolved in a polymeric matrix.

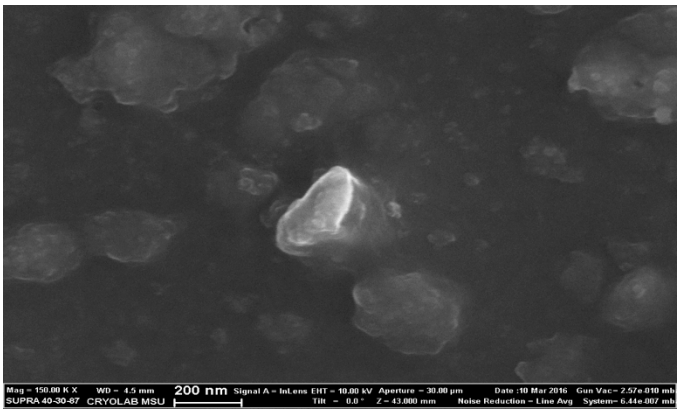

Figure 1. SEM image of nc-Si(1)/poly-3(hexylthiophene) (P3HT) samples.

Raman spectra were similar for both types of samples. The Raman spectrum of the nc-Si(2)/P3HT samples is shown in Figure 2. According to the literature data, the peak near 430 and 520 cm^{-1} in the Raman spectrum corresponds to the C–C deformation mode of the polymer and silicon nanocrystals [11,18], respectively; the peak near 728 cm^{-1} corresponds to an antisymmetric C–S–C ring skeleton deformation in the thiophene ring of the polymer [19]; and the peak near 1390 and 1450 cm^{-1} can be assigned to the C–C skeletal stretch mode and the C=C symmetric stretch mode of the polymer, respectively [20,21]. The other less intense peaks observed in the wavenumber range of 570, 850, 1000, 1100, 1150, 1250 and 1525, 1560 cm^{-1} can be assigned to the C–C rotational mode, C=C deformation mode, C–C stretching mode [21], the C–H bending mode [22], the C–C symmetric stretching mode [23], a combination of the C–C stretching and the C–H stretching mode [21,24,25] and the C = C antisymmetric stretch mode [20,23], respectively. Thus, according to Figure 2, the Raman spectrum consists of lines caused by a polymeric matrix and also a poorly resolved peak, which is characteristic of silicon nanocrystals. The results of a Raman investigation confirmed the data of electronic microscopy, showing that all samples under investigation represent the non-uniform structure of a polymeric matrix with the silicon nanoparticles dissolved in it.

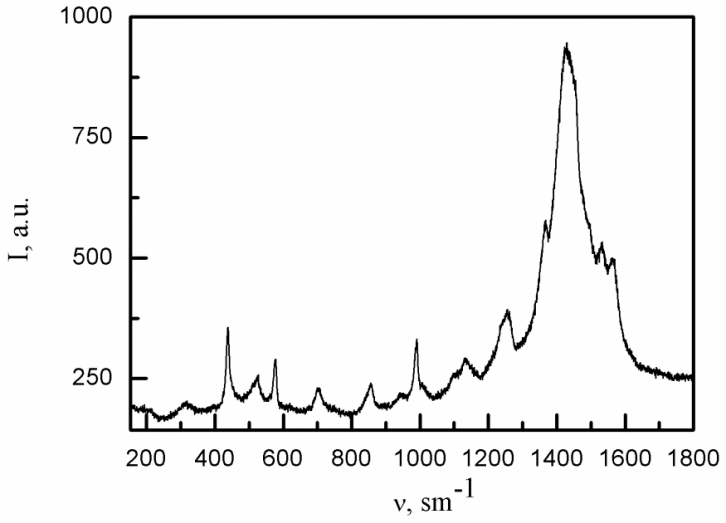

Figure 2. Raman spectrum of the nc-Si(2)/P3HT samples.

For the direct detection of the separation processes of photoinduced charges in the nc-Si/P3HT structures, the EPR-spectroscopy technique was used. In Figure 3a, the EPR spectra of nc-Si(1)/P3HT samples in the dark and under illumination are presented.

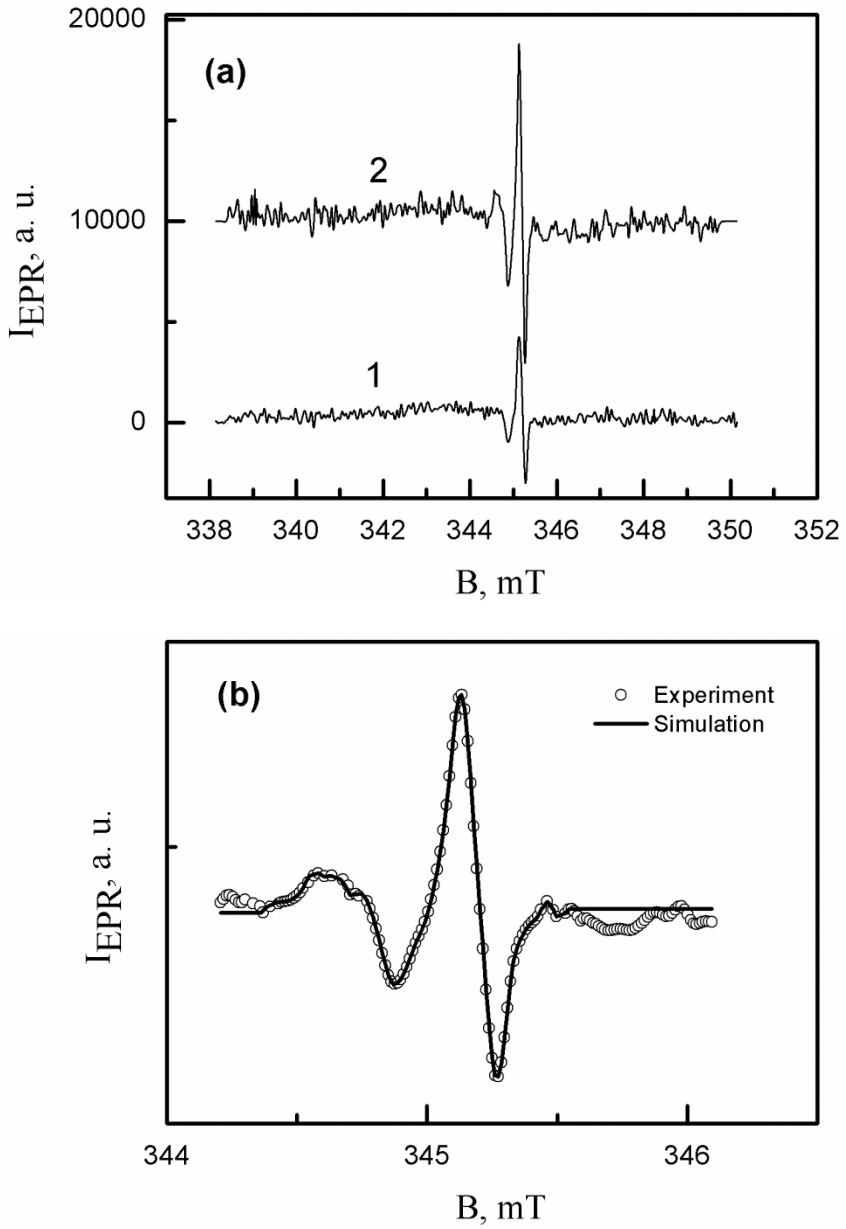

Figure 3. (**a**) EPR spectra of nc-Si(1)/P3HT samples in the dark (1) and under illumination (2). (**b**) Experimental and simulated EPR signals of nc-Si(1)/P3HT samples.

The EPR spectra are characterized by two overlapped signals: one is poorly resolved, with a g-factor equal to 2.0050 originating from the silicon dangling bonds [26], while the second one has an anisotropic form and is described by the following parameters: $g_1 = 2.0030$, $g_2 = 2.0022$, $g_3 = 2.0013$, extracted from computer simulation. The result of the computer simulation is shown in Figure 3b. According to the literature data, this EPR signal can be attributed to the positive polarons in P3HT [9,21]. Under illumination, an amplitude of a polaron EPR signal increases, pointing to the separation process of photoexcited charge carriers. To be sure that the positive polarons are localized in P3HT, we have investigated these structures separately. In Figure 4a, the EPR spectra for P3HT samples in similar conditions are shown, both in the dark and under illumination.

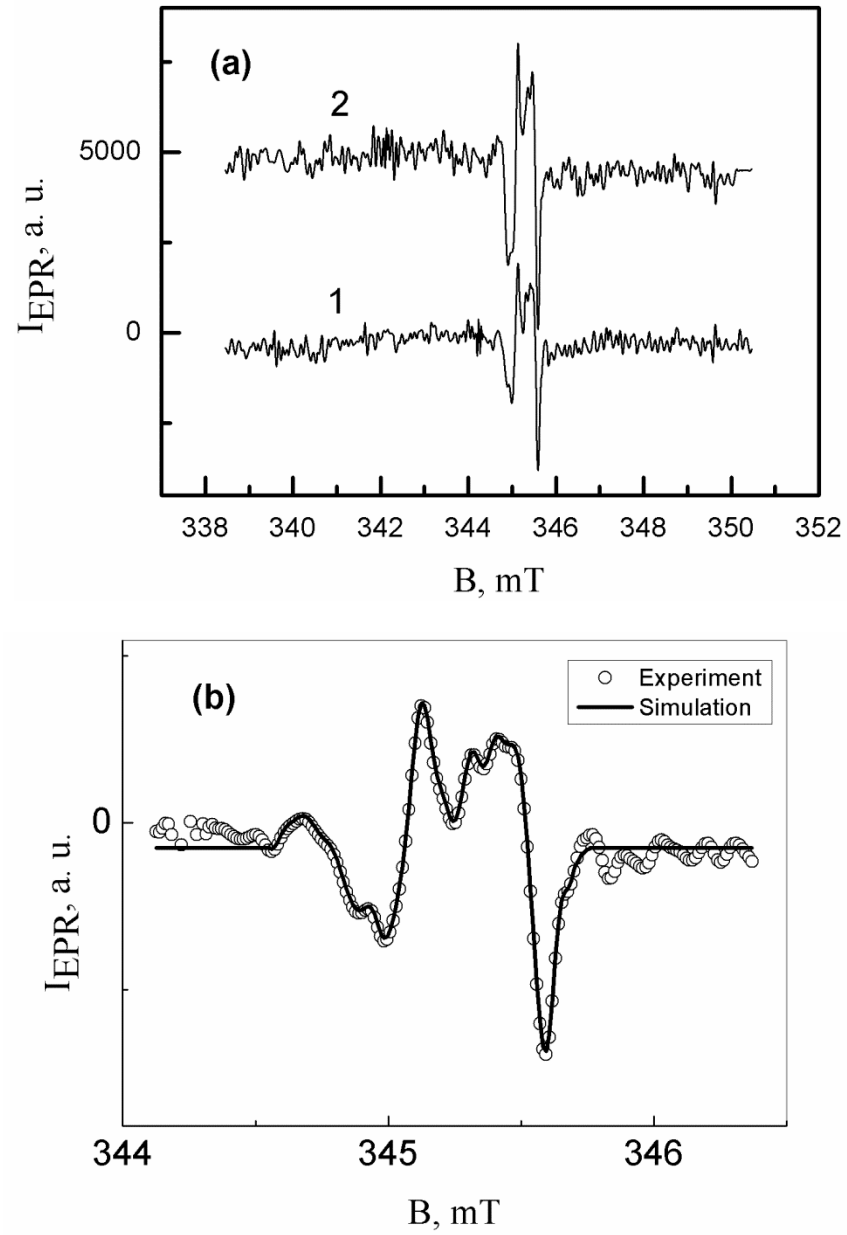

Figure 4. (**a**) EPR spectra of P3HT samples in the dark (1) and under illumination (2). (**b**) Experimental and simulated EPR signals of P3HT samples.

According to the computer simulation, the EPR spectrum consists of two EPR signals with parameters that differ slightly: EPR(I) g_1 = 2.0028, g_2 = 2.0019, g_3 = 2.0009 and EPR(II) g_1 = 2.0031, g_2 = 2.0021, g_3 = 2.0012. The result of the computer simulation is shown in Figure 4b. The values of the g-factors show the polaron nature of the EPR-centers [9,21]. Probably, we observe the polarons in two different orientations. Thus, data from the EPR spectroscopy are direct proof of the formation of polarons in nc-Si/P3HT structures as a result of the separation of charge carriers with the subsequent localization of a hole in P3HT. Note that this process takes place under the conditions of indoor light and are amplified under additional illumination.

The silicon nanoparticles was measured for a comparison of the defects' natures and properties. Figure 5 shows the EPR spectra measured under dark conditions and in the presence of illumination.

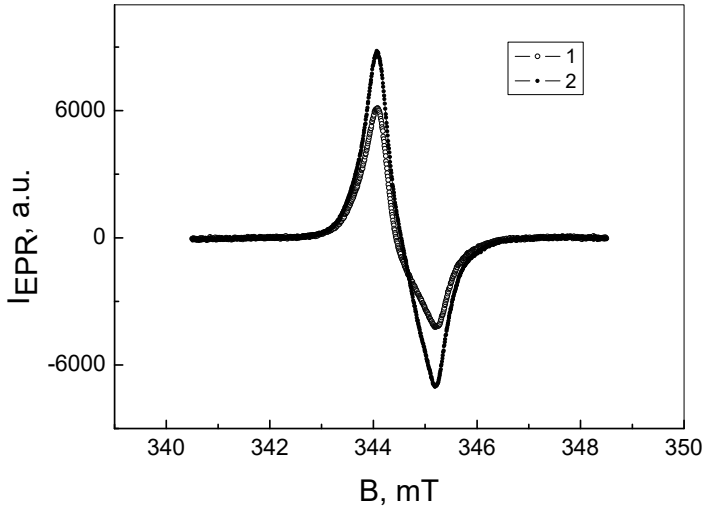

Figure 5. EPR spectra of nc-Si(1) in the dark (1) and under illumination (2).

As follows from the presented data, the EPR spectrum has an anisotropic structure. The following values of the g-tensor were obtained from computer simulation: $g_1 = 2.0021$, $g_2 = 2.0088$. The EPR signal with these anisotropic parameters can be attributed to the paramagnetic centers, which are P_b centers (a silicon dangling bond at the Si/SiO_2 interface) according to the literature data [27,28]. Therefore, an oxidation of silicon nanoparticles takes place in air. Under illumination, the intensity of the EPR spectrum increases. The effect of illumination was reversible, showing recharge processes in the samples.

For the determination of the photovoltaic parameters of the samples and qualitative evaluation of the effectiveness of solar energy conversion, the current density–voltage (abbreviated as current–voltage [8,9]) characteristics were measured (Figure 6). White light illumination was used with an intensity of 50 mW/cm^2. As can be seen from Figure 6, nc-Si(1)/P3HT samples have a higher open-circuit voltage (0,2 V) than nc-Si(2)/P3HT samples (0,16 V). Although these open-circuit voltage values are not a record, it is possible in principle to use nc-Si/P3HT samples for photoconversion.

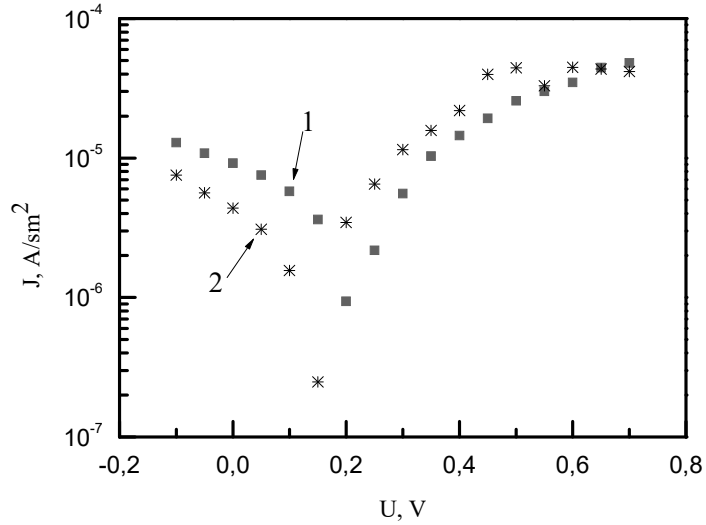

Figure 6. Current–voltage characteristics of the studied samples. Dependence 1—nc-Si(1)/P3HT samples; dependence 2—nc-Si(2)/P3HT samples.

Although the efficiency of the solar energy conversion of the samples in our study was low (not exceeding 5%), we have demonstrated that EPR spectroscopy is an effective tool for the detection of polarons in nc-Si/P3HT prepared by different techniques.

4. Conclusions

The structures consisting of P3HT polymer and silicon nanoparticles, in which silicon nanoparticles are prepared by electrochemical etching and the laser ablation of single-crystal silicon, have the possibility of converting solar energy into electric energy. In nc-Si samples, P_b centers are present according to the EPR data. A lack of P_b centers in the nc-Si/P3HT structures evidences an absence of oxygen in the samples. Positive polarons are detected in P3HT samples. Using EPR spectroscopy, it has been found that it is possible to detect the separation of photoexcited charge carriers in nc-Si/P3HT samples prepared both by the electrochemical etching of a silicon single crystal in hydrofluoric acid solution and by using the laser ablation of single-crystal silicon in organic solvents. The obtained data is useful for solar energy application since they demonstrate the possibility of the preparation of solar cell samples using simple and cheap methods of sample synthesis (for example, the electrochemical etching of silicon monocrystals).

This work was supported by the Russian Foundation for Basic Research (Grant No 18-29-23005).

Author Contributions: Conceptualization, E.A.K. and P.A.F.; Methodology, E.A.K.; Software, A.S.V.; Validation, E.A.K. and A.S.V.; Formal Analysis, P.A.F.; Investigation, E.A.K., A.S.V. and P.A.F.; Resources, A.S.V.; Data Curation, E.A.K.; Writing-Original Draft Preparation, E.A.K.; Writing-Review & Editing, E.A.K., A.S.V. and P.A.F.; Visualization, P.A.F.; Supervision, E.A.K.; Project Administration, A.S.V.; Funding Acquisition, P.A.F.

Funding: This research was funded by the Russian Foundation for Basic Research Grant number 18-29-23005.

Conflicts of Interest: The authors declare no conflict of interest.

References

1. Kazmerski; Lawrence, L. Photovoltaics: A review of cell and module technologies. *Renew. Sustain. Energy Rev.* **1997**, *1*, 71–170. [CrossRef]
2. Meyer, P.V. Technical and economic optimization for CdTe PV at the turn of the millennium. *Prog. Photovolt. Res. Appl.* **2000**, *8*, 161–169. [CrossRef]
3. Rau, U.; Schock, H.W. Cu(In, Ga)Se2 solar Cells. Clean Electricity from Photovoltaics. *Ser. Photoconvers. Solar Energy* **2001**, *1*, 277–345.
4. Gremenok, V.F.; Tivanov, M.S.; Zalesski, V.B. Solar cells based on semiconductors. *Int. Sci. J. Altern. Energy Ecol.* **2009**, *69*, 59–124.
5. Emelyanov, A.V.; Khenkin, M.V.; Kazanskii, A.G.; Forsh, P.A.; Kashkarov, P.K.; Gecevicius, M.; Beresna, M.; Kazansky, P.G. Femtosecond laser induced crystallization of hydrogenated amorphous silicon for photovoltaic applications. *Thin Solid Films* **2014**, *556*, 410–413. [CrossRef]
6. Best Research-Cell Efficiencies. Available online: https://www.nrel.gov/pv/assets/pdfs/best-research-cell-efficiencies-190416.pdf (accessed on 25 April 2019).
7. Hemaprabhaa, E.; Pandeya, U.K.; Chattopadhyaya, K.; Ramamurthya, P.C. Doped silicon nanoparticles for enhanced charge transportation in organic inorganic hybrid solar cells. *Solar Energy* **2018**, *173*, 744–751. [CrossRef]
8. Salikhov, R.B.; Biglova, Y.N.; Yumaguzin, Y.M.; Salikhov, T.R.; Mustafin, A.G. Solar photoconverters based on thin films of organic materials. *Tech. Phys. Lett.* **2013**, *39*, 854–859. [CrossRef]
9. Niesar, S.; Dietmueller, R.; Nesswetter, H.; Wiggers, H.; Stutzmann, M. Silicon/organic semiconductor heterojunction for solar cells. *Phys. Stat. Sol. A.* **2009**, *206*, 2775–2781. [CrossRef]
10. Shao, M.; Keum, J.; Chen, J.; He, Y.; Chen, W.; Browning, J.F.; Jakowski, J.; Sumpter, B.G.; Ivanov, I.N.; Ma, Y.-Z.; et al. The Isotopic Effects of Deuteration on Optoelectronic Properties of Conducting Polymers. *Nat. Commun.* **2014**, *5*, 3180. [CrossRef]
11. Liu, C.-Y.; Holman, Z.C.; Kortshagen, U.R. Hybrid solar cells from P3HT and silicon nanocrystals. *Nano Lett.* **2009**, *9*, 449–456. [CrossRef]
12. Kaftelen, H.; Ocakoglu, K.; Thomann, R.; Tu, S.Y.; Weber, S.; Erdem, E. EPR and photoluminescence spectroscopy studies on the defect structure of ZnO nanocrystals. *Phys. Rev. B* **2012**, *86*, 014113-1–014113-9. [CrossRef]

13. Erdem, E. Microwave power, temperature, atmospheric and light dependence of intrinsic defects in ZnO nanoparticles: A study of electron paramagnetic resonance (EPR) spectroscopy. *J. Alloy. Compd.* **2014**, *605*, 34–44. [CrossRef]
14. Von Bardeleben, H.J.; Ortega, C.; Grosman, A.; Morazzani, V.; Siejka, J.; Stievenard, D. Defect and structure analysis of n^+-, p^+- and p-type porous silicon by the electron paramagnetic resonance technique. *J. Lumin.* **1993**, *57*, 301–313. [CrossRef]
15. Riikonen, J.; Salomaki, M.; van Wonderen, J.; Kemell, M.; Xu, W.; Korhonen, O.; Ritala, M.; MacMillan, F.; Salonen, J.; Lehto, V.-P. Surface chemistry, reactivity and pore structure of porous silicon oxidized by various methods. *Langmuir* **2012**, *28*, 10573–10583. [CrossRef]
16. Demin, V.A.; Konstantinova, E.A.; Kashkarov, P.K. Luminescence and photosensitization properties of ensembles of silicon nanocrystals in terms of an exciton migration model. *J. Exp. Theor. Phys.* **2010**, *111*, 830–843. [CrossRef]
17. Stoll, S.; Schweiger, A. EasySpin, a comprehensive software package for spectral simulation and analysis in EPR. *J. Magn. Reson.* **2006**, *178*, 42–55. [CrossRef] [PubMed]
18. Emelyanov, A.; Kazanskii, A.; Kashkarov, P.; Konkov, O.; Terukov, E.; Forsh, P.; Khenkin, M.; Kukin, A.; Beresna, M.; Kazansky, P. Effect of the femtosecond laser treatment of hydrogenated amorphous silicon films on their structural, optical, and photoelectric properties. *Semiconductors* **2012**, *46*, 749–754. [CrossRef]
19. Falke, S.; Eravuchira, P.; Maternyb, A.; Lienaua, C. Raman spectroscopic identification of fullerene inclusions in polymer/fullerene blends. *J. Raman Spectrosc.* **2011**, *42*, 1897–1900. [CrossRef]
20. Motaung, D.E.; Malgas, G.F.; Nkosi, S.S.; Mhlongo, G.H.; Mwakikunga, B.W.; Malwela, T.; Arendse, C.J.; Muller, T.F.G.; Cummings, F.R. Comparative study: The effect of annealing conditions on the properties of P3HT:PCBM blends. *J. Mater. Sci.* **2013**, *48*, 1763–1778. [CrossRef]
21. Konkin, A.; Roth, H.-K.; Scharff, P.; Aganov, A.; Ambacher, O.; Sensfuss, S. K-band ESR studies of structural anisotropy in P3HT and P3HT/PCBM blend polymer solid films: Paramagnetic defects after continuous wave Xe-lamp photolysis. *Solid State Commun.* **2009**, *149*, 893–897. [CrossRef]
22. Saini, V.; Li, Z.R.; Bourdo, S.; Dervishi, E.; Xu, Y.; Ma, X.D.; Kunets, V.P.; Salamo, G.J.; Viswanathan, T.; Biris, A.R.; et al. Electrical, optical, and morphological properties of P3HT-MWNT nanocomposites prepared by in situ polymerization. *J. Phys. Chem. C* **2009**, *113*, 8023–8029. [CrossRef]
23. Baibarac, M.; Lapkowski, M.; Pron, A.; Lefrant, S.; Baltog, I. SERS spectra of poly (3-hexylthiophene) in oxidized and unoxidized states. *J. Raman Spectrosc.* **1998**, *29*, 825–832. [CrossRef]
24. Louarn, G.; Trznadel, M.; Buisson, J.P.; Laska, J.; Pron, A.; Lapkowski, M.; Lefrant, S. Raman spectroscopic studies of regioregular poly (3-alkylthiophenes). *J. Phys. Chem.* **1996**, *100*, 12532–12539. [CrossRef]
25. Klimov, E.; Li, W.; Yang, X.; Hoffmann, J.G.; Loos, G. Scanning Near-Field and Confocal Raman Microscopic Investigation of P3HT-PCBM Systems for Solar Cell Applications. *Macromolecules* **2006**, *39*, 4493–4496. [CrossRef]
26. Emelyanov, A.V.; Konstantinova, E.A.; Forsh, P.A.; Kazanskii, A.G.; Khenkin, M.V.; Petrova, N.N.; Terukov, E.I.; Kirilenko, D.A.; Bert, N.A.; Konnikov, S.G.; et al. Features of the structure and defect states in hydrogenated polymorphous silicon films. *JETP Lett.* **2013**, *97*, 466–469. [CrossRef]
27. Cantin, J.L.; Schoisswohl, M.; Von Bardeleben, H.J. Electron-paramagnetic-resonance study of the microscopic structure of the Si(001)-SiO_2 interface. *Phys. Rev. B.* **1995**, *52*, R11599–11602. [CrossRef]
28. Minnekhanov, A.A.; Konstantinova, E.A.; Pustovoi, V.I.; Kashkarov, P.K. The Influence of the Formation and Storage Conditions of Silicon Nanoparticles Obtained by Laser-Induced Pyrolysis of Monosilane on the Nature and Properties of Defects. *Tech. Phys. Lett.* **2017**, *43*, 424–427. [CrossRef]